IOP Publishing Semiconductor Science and Technology
Semicond. Sci. Technol. **35** (2020) 075004 (6pp) https://doi.org/10.1088/1361-6641/ab7e44

Evolution of the surface states during the *in situ* SiN layer formation on AlN/GaN heterostructures

K Zhuravlev[1,2,4], V Mansurov[1], Yu Galitsyn[1], T Malin[1], D Milakhin[1,4] and V Zemlyakov[3]

[1] Department of Physics and Engineering of Semiconductor Structures, Rzhanov Institute of Semiconductor Physics Siberian Branch of Russian Academy of Sciences, Novosibirsk, Russia
[2] Department of Physics, Novosibirsk State University, Novosibirsk, Russia
[3] National Research University of Electronic Technology «MIET», Zelenograd, Moscow, Russia

E-mail: zhur@isp.nsc.ru and dmilakhin@isp.nsc.ru

Received 25 November 2019, revised 26 February 2020
Accepted for publication 10 March 2020
Published 28 May 2020

Abstract

The effect of a monolayer thick SiN film on the surface states of the AlN/GaN heterostructure grown by molecular beam epitaxy was investigated. It was revealed that the submonolayer SiN coating of the AlN surface leads to the formation of an ordered $(\sqrt{3} \times \sqrt{3})R30°$ structure. Further SiN film growth results in a Si-enriched SiN amorphous film formation. The Fermi level, pinned 1 eV above the valence band maximum of as-grown AlN, jumps 2.3 eV when $(\sqrt{3} \times \sqrt{3})R30°$ is formed, and then gradually goes to 3.1 eV with an increase in the thickness of the SiN film up to four monolayers. This is explained by the evolution of surface states, as well as the appearance of donor-like states in a Si-enriched SiN film. The presence of donor-like states was confirmed when studying the effect of current collapse in enhancement-mode high electron mobility transistors made of SiN/AlN/GaN heterostructures.

Keywords: surface states, AlN/GaN heterostructure, SiN-passivation, GaN-enhancement-mode high electron mobility transistor (E-HEMT), current collapse

(Some figures may appear in colour only in the online journal)

1. Introduction

Devices based on the Al(Ga)N/GaN heterojunction with two-dimensional electron gas (2DEG) are excellent candidates to replace Si-based high-power as well as high-frequency power AlGaAs/InGaAs devices owing to the superior electrical and transport properties, such as high 2DEG sheet charge density ($\sim 1-3 \times 10^{13}$ cm^{-2}) and high electron saturation drift velocities $\sim 2.5 \times 10^{7}$ cm s^{-1}, of these III-nitride heterostructures.

The importance of surface donor states as a source of electrons for the 2DEG formation in Al(Ga)N/GaN heterostructure was highlighted in the works of Smorchkova *et al* [1] and Ibettson *et al* [2] to explain the 2DEG electron density behavior as a function of barrier thickness. A review and critical analysis of different kinds (acceptors and donors) of the surface states distributions and its role in 2DEG formation was recently presented by Bakeroot *et al* [3] and Ber *et al* [4]. It was underlined that the origin of 2DEG in AlGaN/GaN heterostructures still remains a conundrum although there seems to be a consensus that donor states at the surface (or states at the interface with a dielectric film in the case of surface passivation) play a significant role. Several groups attribute the very existence of 2DEG to the presence of donor-like surface states. On the other hand, it is widely discussed the negative impact of surface states on the performance of AlGaN/GaN high electron mobility transistors (HEMTs) because of the gate leakage and current collapse phenomena connected with the trapping of electrons by surface states [5–7]. Although, for the reasons of simplicity, discrete donor state on the surface has been discussed in many papers [1, 2], possibility of distribution of interface states was not excluded [3, 8]. However, hitherto there are very little experimental researches on the nature of surface donor and acceptor states in Al(Ga)N/GaN HEMTs.

[4] Author to whom any correspondence should be addressed.

Moreover, the role of the passivation film in the modification (generation and elimination) of various types of surface states is unclear.

AlN/GaN HEMTs are very attractive for high-frequency power amplifiers and high voltage power switches [9–13] because of the best dielectric properties of AlN [14], the higher concentration of electrons in 2DEG and the possibility to reduce gate-2DEG channel distance. However, the high AlN surface sensitivity to oxidation and contamination leads to problems such as current collapse and large leakage current, limiting the device performance and reliability. In many cases passivation films are deposited *ex situ* onto the surface of the AlGaN/GaN heterostructure, but this does not solve the problem of oxidation and contamination [15–17]. The *in situ* deposition of the SiN film immediately after the growth of the transistor structure prevents the direct exposure of AlN surface to air improving HEMTs performances [18]. This method was used in metal-organic chemical vapor deposition, where a high growth temperature can promote the formation of high-quality SiN films. However, little is known about the prospects of this method in molecular beam epitaxy (MBE). Meanwhile, MBE allows careful study of the SiN formation process.

In this paper, we report a study on the *in situ* formation of a silicon nitride film on the surfaces of AlN/GaN heterostructures grown by ammonia MBE. The nature and evolution of surface states during the formation of a passivating SiN film on AlN/GaN heterostructures are discussed.

2. Methods

AlN/GaN heterostructures were grown by molecular-beam epitaxy on 2 inch (0001)-oriented sapphire substrates in a Riber CBE-32 machine. High-purity ammonia additionally cleaned by filter served as the source of active nitrogen. As the sources of group-III metals an aluminum cold lip source with cold neck PBN crucible and gallium double zone source with PG crucible were used. For minimization of contamination, the substrates were annealed at a temperature $T = 600$ °C for several hours in the loading dock before they were introduced onto the sample holder into the growth chamber. The substrate temperature was controlled by an infrared pyrometer. Before growing the heterostructure, the substrates were additionally annealed in the growth chamber at $T = 900$ °C, then it was nitridated in an ammonia flow of $F = 25$ sccm for 10 min at $T = 840$ °C and was covered by AlN nucleation layer at a low-temperature (600 °C) [19]. The deposition of such nucleation layer in an Al-rich ambient imparts GaN and AlN layers with metal-polarity. Next, a 300-nm thick AlN buffer, 1.5 μm thick GaN buffer and about 3 nm thick AlN barrier layers were grown at *T/F* = 940 °C/15 sccm, 800 °C/150 sccm and 830 °C/150 sccm, respectively. The growth rate of AlN was calibrated by x-ray diffraction, Raman spectroscopy and transmission electron microscopy of short-period AlN-GaN multiple quantum well structures [20]. The ultrathin silicon nitride dielectric film was deposited at 500 °C–900 °C in ammonia and silane flows, directly following the growth of the AlN barrier layer in the same MBE chamber. The formation of an ultrathin SiN film on the surface of an AlN (300 nm) layer and AlN/GaN heterostructure (3 nm 1500 nm^{-1}) was studied. SiN films were deposited at various gas fluxes containing 0.7% SiH_4 in N_2 (1.5–6 sccm) and NH_3 (10–50 sccm) and different substrate temperatures (500 °C–900 °C).

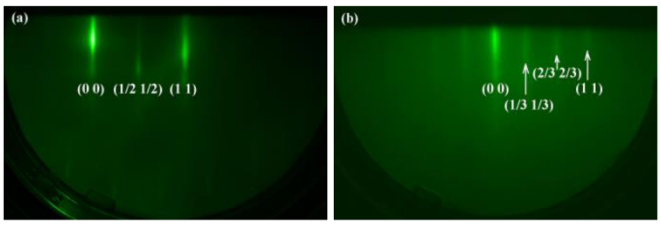

Figure 1. RHEED patterns of the (0001)AlN surface (a) the (2 × 2) structure of the initial surface at $T = 500$ °C; (b) the ($\sqrt{3} \times \sqrt{3}$) R30° structure after exposure to silane and ammonia at $T = 900$ °C.

The reflection high-energy electron diffraction (RHEED) with a primary electron beam energy of 11 keV was used to *in situ* study the formation of a silicon nitride film. To determine the composition and thickness of the dielectric film, x-ray photoelectron spectroscopy (XPS) was performed. Samples were grounded to the basis level of the XPS apparatus to ensure that the origin of binding energy in XPS spectra corresponds to the Fermi level of the samples. Hall measurements using the van der Pauw method in a 0.5 T magnetic field on the SiN/AlN/GaN structures showed a sheet carrier densities of 1.3×10^{13} cm^{-2} and a mobility of 1200 cm^2·V^{-1} s^{-1} at room temperature. For the fabrication of HEMT, mesa isolation was carried out using CCl_4 plasma reactive ion etching, and the Si_3N_4 layer was applied by plasma deposition to protect the AlN surface during thermal annealing of ohmic contacts. The ohmic contacts were formed by rapid thermal annealing at 850 °C for 30 s in a nitrogen atmosphere of the Ti/Al/Ni/Au metal stack deposited by the electron beam evaporator. The Ni/Au gate of the transistor had a 0.6 μm length and 50–400 μm width. Before the gate was formed, the specific drain-source current (I_D) was about $I_D = 1$ A · mm^{-1}, and after the gate was formed, the I_D value dropped to zero. For a positive gate bias +3 V the I_D value reaches 0.5 A · mm^{-1}. These enhancement-mode HEMTs (E-HEMTs) exhibit a transconductance of 350 mS · mm^{-1} and a breakdown voltage of 60 V [21]. The dependence of the drain current on the drain voltage was measured using a BILT/IVCAD characterization pulse system consisting of mainframes, input and output pulsers, and IVCAD measurement and modeling characterization software. Input and output pulsers designed to bias the gate and drain, respectively.

3. Results and discussion

First the evolution of the RHEED pattern of the AlN surface during the deposition of a SiN film was analyzed. Figure 1 shows the diffraction patterns for the azimuth direction of [1–100] taken at key stages of the process. At the freshly grown AlN surface, a (2 × 2) reconstruction was observed (figure 1(a)), when the sample was cooled below 600 °C under

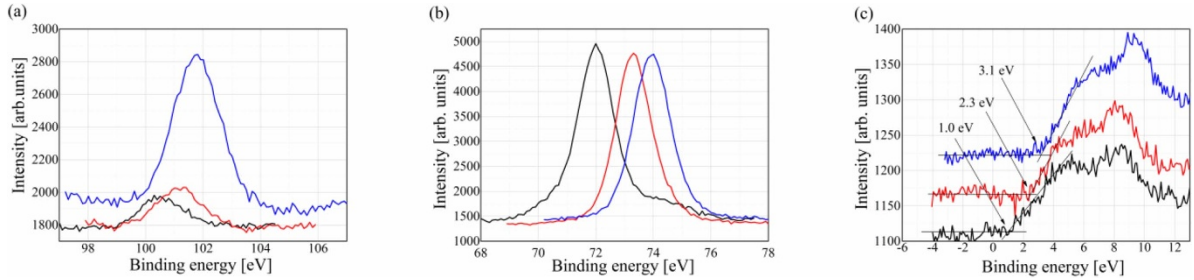

Figure 2. XPS spectra acquired at different Si_3N_4 exposure doses (black–lowest dose $D_1 = 6$ sccm · min, red–middle dose $D_2 = 60$ sccm · min, blue–highest dose $D_3 = 720$ sccm · min) (a) Si2p core level; (b) Al2p core level; (c) the AlN valence band with respect to Fermi level.

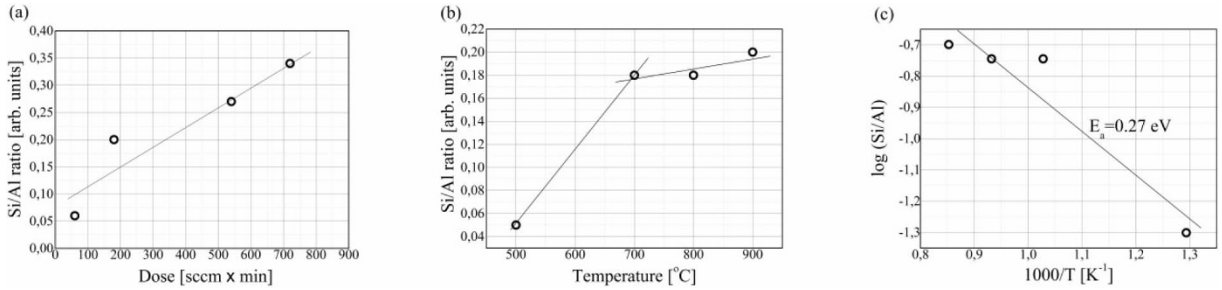

Figure 3. The ratio of the Si/Al XPS peak area (a) dose dependence at a fixed temperature $T = 900$ °C; (b) temperature dependence at a fixed dose; (c) Arrhenius plot.

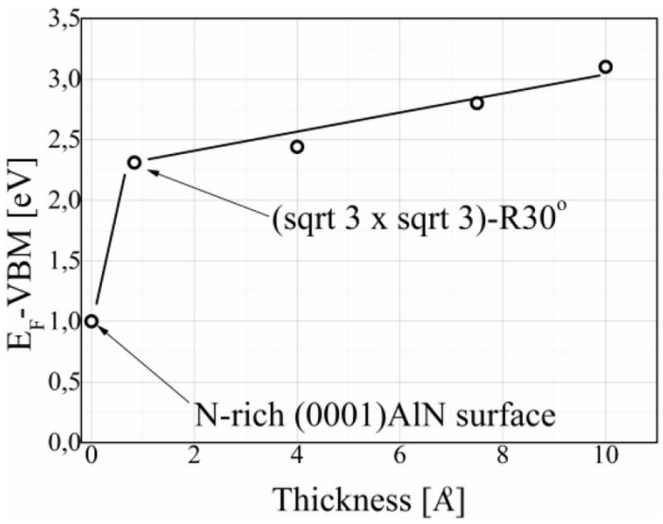

Figure 4. The position of the binding energy of the valence band maximum as a function of the SiN thickness at $T = 900$ °C.

the ammonia flux. The (2 × 2) reconstruction is characteristic for N-rich surfaces of III-nitrides with metallic polarity [22–25]. The co-adsorption of silane and ammonia molecules on the surface of the AlN layer at relatively low substrate temperatures of 500 °C–700 °C leads to the disappearance of the (2 × 2) structure. The intensity of the fundamental spots is weakened and the intensity of the background increases. It means that a disordered adsorption phase appears on the surface, but SiN film is not detected either by RHEED or XPS techniques. The exposure of the fresh AlN surface under the silane and ammonia flux at a higher substrate temperature (700 °C–900 °C) for 20 min leads to formation of a new ordered $(\sqrt{3} \times \sqrt{3})R30°$ structure (figure 1(b)).

The $(\sqrt{3} \times \sqrt{3})R30°$ structure was often observed on the (111) surface of cubic crystals and on the (0001) surface of hexagonal crystals upon adsorption in the simplest case of 1/3 or 2/3 monolayers of different species [26]. Then it is reasonable to assume that the observation of $(\sqrt{3} \times \sqrt{3})R30°$ structure indicates a submonolayer coverage of the AlN surface by the SiN. This assumption is supported by XPS measurements (synthesized later in figure 3). Further exposure of the $(\sqrt{3} \times \sqrt{3})R30°$ reconstructed surface under the silane and ammonia fluxes at high temperature leads to the fading away of the fractional streaks, a gradual decrease in the intensity of the fundamental spots, and an increase of the background intensity. As a result, a diffused (1 × 1) diffraction pattern appears that corresponds to the formation of an ultrathin (several monolayers) film of amorphous silicon nitride on the AlN surface.

Then the changes in the XPS spectrum of the AlN surface during the SiN film deposition were studied. Figure 2 provides evidence that the XPS spectra of the AlN surface lies within the energy range of the Si2p and Al2p signals as well as of the AlN valence band. The exposure dose (D) is defined here as the product of the SiH_4 flux value (F, sccm) and the deposition time (t, min).

The SiN layer thickness on the AlN surface was estimated from the areas of the Si2p and Al2p peaks, taking into account the mean escape depth of the corresponding characteristic photoelectrons, and the exponential decay of the XPS signals with depth. The SiN thickness increases with increasing exposure

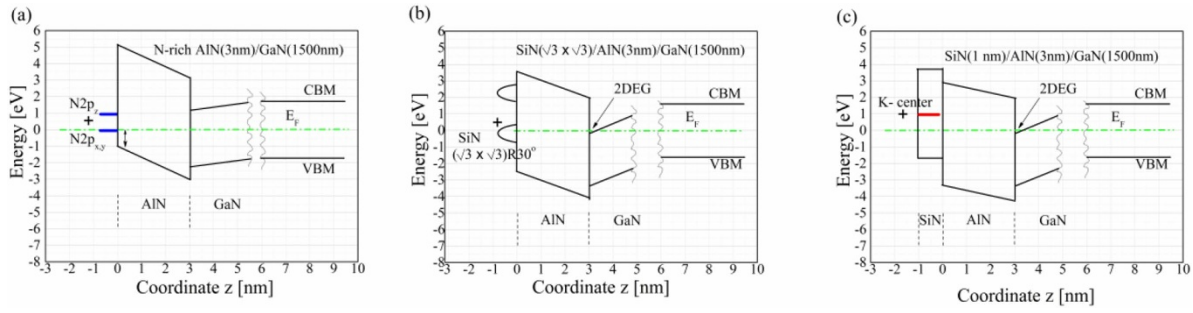

Figure 5. Valence and conduction band potentials against the (0001) growth direction (a) N-rich AlN surface; (b) SiN($\sqrt{3} \times \sqrt{3}$)R30°/AlN/GaN heterostructure; (c) SiN/AlN/GaN heterostructure.

dose at a fixed temperature (900 °C) in figure 3(a). The thickness of the amorphous SiN film with highest deposition dose of 720 sccm·min at 900 °C was estimated as 10–12 Å. On the other hand, the SiN thickness also increases with an increase in the substrate temperature at a fixed dose (figure 3(b)). This behavior corresponds to the normal activation kinetics of chemical reactions between the dissociativly chemisorbed silane and ammonia molecules on the AlN surface. We have estimated the effective activation barrier for the SiN formation as ~0.27 eV from the Arrhenius plot (figure 3(c)). A low value of the activation barrier, most likely, means that the value does not correspond to the activation energy of any real elementary reaction, but it effectively describes a multistep process as a whole.

The composition of the finally formed SiN film was determined using the ratio of the peak area N1 s/Si2p, taking into account the sensitivity factors of the elements. The N/Si ratio turned out to be 1.28 instead of 1.33, characteristic of Si_3N_4, which means that the SiN film is enriched with silicon.

The XPS spectra show (see figure 2) that the Si2p and Al2p atomic states and the valence band maximum (VBM) binding energy shift relative to the Fermi level position with increasing SiN coating thickness on the AlN surface from the submonolayer to about four monolayers. The atomic core levels binding energies shift from 100.3 eV to 102 eV for the Si2p state and from 72.0 eV to 74.0 eV for the Al2p state. The VBM position was measured by linear extrapolation of the high energy side of the valence-band spectrum. The VBM position moved from the initial value of 1 eV up to about 3.1 eV at a thickness SiN of about 10 Å. The dependence of E_F-VBM on SiN thickness is shown in figure 4. A spike in the VBM position associated with the ($\sqrt{3} \times \sqrt{3}$)R30° structure formation is clearly seen in the figure. A further increase in the E_F -VBM value is associated with an increase in the amorphous SiN film thickness.

Let us discuss these issues in more detail. As grown AlN surface, before the SiN deposition, was kept under ammonia flux, and hence the N-rich conditions are realized on the surface. Under the N-rich conditions an *ab initio* calculated N-adatom model as the most stable structure of the (0001)AlN surface was proposed by Northrup *et al* [27] and later supported by Miao *et al* [28]. Three surface bands originate from the N2p (p_x, p_y, p_z) orbitals at energy position of 1–2 eV above the AlN VBM were found. We assume that the initial surface location of the Fermi level (E_F) at 1 eV above VBM is defined by these N-adatoms related donor-like surface states originate from N2p (p_x, p_y) orbitals. The simplified band potential diagram along the growth direction of AlN/GaN for that case is shown in figure 5(a). To construct out this band diagram it was assumed that layers are undoped (intrinsic) semiconductor and uniform electrical fields originate from plane sheets of charges on the surface AlN and AlN/GaN interface.

The synchronous increase of the binding energies of Al2p, Si2p core levels and correspondent shift in the VBM position, when the SiN thickness reaches approximately one monolayer, is associated with a change in the band bending on the sample surface, which is resulted from surface modification. The Fermi level position at about of 2.3 eV above VBM of AlN, induced by the ($\sqrt{3} \times \sqrt{3}$)R30° SiN structure formation (figure 5(b)), corresponds to the first step of the surface state transformation. Surface coverage with the ordered SiN submonolayer is accompanied by the appearance of electronic states approximately 0.9 eV above the VBM position in bulk Si_3N_4 that in turn expected to be about 1.4 eV above the AlN VBM position [29]. We believe that these states are associated with the formation of a new periodic structure of silicon nitride on the AlN surface that differs from the bulk Si_3N_4. Recently, Rosa *et al* have shown by *ab initio* calculations that silicon atoms adsorption on the GaN(0001) surface gives rise to surface states in the GaN band gap [30], Kempisty *et al* have shown that surface states in the GaN band gap also appear during the adsorption of NH_3, NH_2 species [31]. Finally, Zhang *et al* have performed calculations of the surface states arising from different amorphous SiN layers formed on the GaN(0001) surface [32]. There is a lack of similar comprehensive works investigating different compositions as well as ordered or disordered structures of silicon nitrides on the AlN (0001) surface that could allow us to unambiguously identify the states laying 2.3 eV higher than VBM of AlN. Moreover, to our knowledge, there are no studies on the formation of the silicon nitride induced ($\sqrt{3} \times \sqrt{3}$)R30° superstructure on both GaN and AlN(0001) surfaces. Further detailed studies of the atomic arrangement of the superstructure ($\sqrt{3} \times \sqrt{3}$)R30° and its electronic states are required to elucidate the nature of states appearing in the band gap of AlN, which determine the Fermi level position in this case.

With further deposition of silicon nitride, the density of states increases and the states spread over in the energy scale as a result of the thicker amorphous SiN layer formation, in close

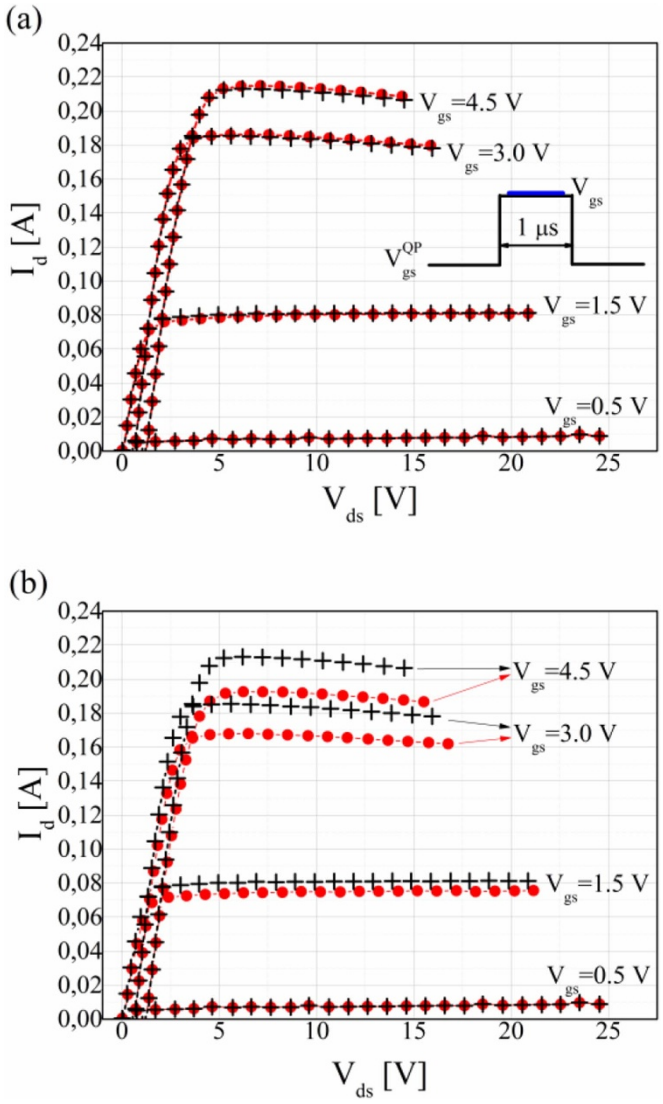

Figure 6. Pulsed current–voltage (*IV*) characteristics of the SiN/AlN/GaN HEMT obtained at different working V_{gs} by sweeping from (a) negative quiescent point ${V_{gs}}^{QP}$ and (b) positive ${V_{gs}}^{QP}$ in comparison with the zero quiescent point. For the *I*–*V* characteristics (a) measured at the quiescent bias points of (${V_{gs}}^{QP} = 0$ V; ${V_{ds}}^{QP} = 0$ V–black crosses) and (${V_{gs}}^{QP} = -3$ V; ${V_{ds}}^{QP} = 0$ V–red circles) ratio between the drain currents is less than 1%, whereas for the *I*–*V* characteristics (b) measured at the quiescent bias points of (${V_{gs}}^{QP} = 0$ V; ${V_{ds}}^{QP} = 0$ V–black crosses) and (${V_{gs}}^{QP} = +3$ V; ${V_{ds}}^{QP} = 0$ V–red circles) ratio between the drain currents is about 6.5% and 9.2% for the $V_{gs} = +1.5$ V and $V_{gs} = +3$ V, respectively. The blue color at the insert of figure (a) indicates an interval of measurements.

analogy to the unified disorder induced gap states (DIGS) model [8], developed to describe the Fermi level pinning on the interfaces of III–V semiconductors with insulators or metals. These transformations of the surface states result in further shift in the position of the Fermi level. Moreover, for the Si-enriched SiN layer, the typically named 'K-centers' appear, as described in references [3, 33, 34]. The K-centers possess donor-like nature and they are connected with Si-atoms dangling bonds in Si_3N_4 layer. These K-centers are associated with energy states located in the middle of the amorphous Si_3N_4 band gap, that is, 2.6 eV above VBM of the bulk Si_3N_4. The donor-like K-centers are placed well above the Fermi level, and hence they stay empty and charged positively (figure 5(c)). The positive charge effectively compensates the negative polarization charge at the AlN surface, therefore a monotonic increase in the E_F-VBM value with an increase in the thickness of the SiN film may be due to an increase in the number of K-centers and/or a modification of the interface states. If the density of the K-centers of amorphous Si_3N_4 became high enough a pinning of E_F occurs at these states [3].

To test the states of the SiN/AlN/GaN heterostructure interface, an E-mode transistor was fabricated [35]. The pulsed current–voltage characteristics of the E-HEMT were measured. In many cases because of the presence of traps the pulsed *IV* characteristics, performed starting from different bias points, are in general different. The HEMT was initially biased at a quiescent bias point (QP) defined by gate and drain bias voltages (${V_{gs}}^{QP}$, ${V_{ds}}^{QP}$), and then pulsed working bias voltages (V_{gs}, V_{ds}) was applied (blue color in figure 6(a)) to make a measurement and record the *IV* characteristics. By setting of different quiescent bias points ${V_{gs}}^{QP}$ and ${V_{ds}}^{QP}$ one can test the gate-source and gate-drain areas, respectively [5]. By setting the sign of the quiescent bias point ${V_{gs}}^{QP}$, it is possible to test traps in selected part of the band gap, and namely, negative/positive gate quiescent biases allow testing the lower/upper part of the band gap, respectively. For example, at zero quiescent biases (${V_{gs}}^{QP} = 0$, ${V_{ds}}^{QP} = 0$) the empty traps do not affect the drain current, the drain current is the highest. At application of negative bias to the gate (${V_{gs}}^{QP} = -$V, ${V_{ds}}^{QP} = 0$) electrons from the gate fill neutral traps below the gate. Traps being negatively charged act as 'virtual gates', reducing drain current during a measurement [6]. On the other hand, on application of positive bias (${V_{gs}}^{QP} = +$ V, ${V_{ds}}^{QP} = 0$) the positively charged traps in upper part of the band gap capture electron from channel, hence, are neutralized. This also causes a decrease in drain current due to an effective decrease in gate bias. Gate and drain voltages are then synchronously pulsed to different amplitudes. We assume that the pulses were shorter than the characteristic time of electron escape from traps therefore the state of traps was defined by the quiescent point and did not change during the application of working pulsed voltages [36, 37].

Figure 6(a) demonstrates pulsed *IV* characteristics measured at working points (V_{gs}, V_{ds}) starting from negative and zero quiescent bias points. The voltage pulse width shown at the insert of figure 6(a) was 1 μs. In this case it was found that the *IV* characteristic at ${V_{gs}}^{QP} = -3$ V does not changed comparing with ${V_{gs}}^{QP} = 0$ V. Hence, the charge state of the traps is the same for the both ${V_{gs}}^{QP}$ (0 and -3 V), therefore, the concentration of traps is very low due to the effect of passivation. At positive quiescent bias ${V_{gs}}^{QP} > 0$ the drain current drops comparing with ${V_{gs}}^{QP} = 0$ V at about 10% as it shown in figure 6(b). This decrease in current is due to the capture of electrons by positively charged centers. We assume that the donor-like K centers are electron traps. This effect should be taken into account when designing the E-mode HEMT on base of passivated SiN/AlN/GaN heterostructures.

4. Conclusion

In this work, we studied the evolution of surface states during the *in situ* SiN formation on the surface of AlN/GaN heterostructures grown by ammonia molecular beam epitaxy. The $(\sqrt{3} \times \sqrt{3})$R30° SiN structure on the AlN surface was observed for the first time. The appearance of a new ordered SiN structure is accompanied by a sharp jump in the AlN valence band maximum from 1 eV to 2.3 eV below the Fermi level, which is most likely due to the formation of new surface states in the AlN band gap. A further increase in the SiN film thickness (up to 10 Å) leads to a gradual shift of the AlN valence band maximum by 3.1 eV below the Fermi level. This shift is the result of the transformation of the spectrum of the surface states as well as appearance and increase of the net concentration of donor-like K-centers in the SiN film enriched with silicon. A E-mode HEMT has been fabricated on the base of the SiN passivated AlN/GaN heterostructure. It was shown that the *in situ* grown SiN film completely eliminates electron traps with energy levels in the lower part of the AlN band gap, while ionized donor-like centers appeared, acting as electron traps from the E-HEMT channel.

Acknowledgments

This work was partly supported by the Russian Foundation for Basic Researches under Grant Nos. 17-02-00947 and 18-52-00008.

ORCID iDs

D Milakhin https://orcid.org/0000-0002-9042-8929
V Zemlyakov https://orcid.org/0000-0001-5681-9603

References

[1] Smorchkova I, Elsass C, Ibbetson J, Vetury R, Heying B, Fini P, Haus E, DenBaars S, Speck J and Mishra U 1999 *J. Appl. Phys.* **86** 4520
[2] Ibbetson J, Fini P, Ness K, DenBaars S, Speck J and Mishra U 2000 *Appl. Phys. Lett.* **77** 250
[3] Bakeroot B, You S, Wu T-L, Hu J, Van Hove M, De Jaeger B, Geens K, Stoffels S and Decoutere S 2014 *J. Appl. Phys.* **116** 134506
[4] Ber E, Osman B and Ritter D 2019 *IEEE Trans. Electron Devices* **66** 2100
[5] Binari S, Ikossi K, Roussos J, Kruppa W, Park D, Dietrich H, Koleske D, Wickenden A and Henry R 2001 *IEEE Trans. Electron Devices* **48** 465
[6] Vetury R, Zhang N, Keller S and Mishra U 2001 *IEEE Trans. Electron Devices* **48** 560
[7] Hasegawa H, Inagaki T, Ootomo S and Hashizume T 2003 *J Vac. Sci. Technol.* B **21** 1844
[8] Hasegawa H and Ohno H 1986 *J. Vac. Sci. Technol.* B **4** 1130
[9] Zimmermann T, Deen D, Cao Y, Simon J, Fay P, Jena D and Xing H 2008 *IEEE Electron Device Lett.* **29** 661
[10] Chabak K *et al* 2011 *IEEE Electron Device Lett.* **32** 1677
[11] Poblenz C, Corrion A, Recht F, Suh C, Chu R, Shen L, Speck J and Mishra U 2007 *IEEE Electron Device Lett.* **28** 945
[12] Wang X, Huang S, Zheng Y, Wei K, Chen X, Zhang H and Liu X 2014 *IEEE Trans. Electron Devices* **61** 1341
[13] Lu X, Ma J, Jiang H and Lau K 2014 *Appl. Phys. Lett.* **105** 102911-1
[14] Shen L, Heikman S, Moran B, Coffie R, Zhang N-Q, Buttari D, Smorchkova I, Keller S, DenBaars S and Mishra U 2001 *IEEE Electron Device Lett.* **22** 457
[15] Hashizume T, Ootomo S and Hasegawa H 2003 *Appl. Phys. Lett.* **83** 2952
[16] Taking S *et al* 2010 *Electron. Lett.* **46** 301
[17] Taking S, MacFarlane D and Wasige E 2011 *IEEE Trans. Electron Devices* **58** 1418
[18] Atmaca G, Narin P, Kutlu E, Malin T, Mansurov V, Zhuravlev K, Lisesivdin S and Özbay E 2018 *IEEE Trans. Electron Devices* **65** 955
[19] Malin T, Milakhin D, Mansurov V, Galitsyn Y, Kozhuhov A, Ratnikov V, Smirnov A, Davydov V and Zhuravlev K 2018 *Semiconductors* **52** 789
[20] Zhuravlev K, Malin T, Trubina S, Erenburg S, Dobos L, Pecz B, Davydov V, Smirnov A and Kyutt R 2013 *Phys. Status Solidi* c **10** 311
[21] Zhuravlev K, Malin T, Mansurov V, Zemlyakov V, Egorkin V and Parnes Y 2016 *Tech. Phys. Lett.* **42** 750
[22] Smith A, Ramachandran V, Feenstra R, Greve D, Shin M-S, Skowronski M, Neugebauer J and Northrup J 1998 *J. Vac. Sci. Technol.* A **16** 1641
[23] Smith A, Feenstra R, Greve D, Shin M, Skowronski M, Neugebauer J and Northrup J 1998 *Appl. Phys. Lett.* **72** 2114
[24] Smith A, Feenstra R, Greve D, Shin M, Skowronski M, Neugebauer J and Northrup J 1999 *Surf. Sci.* **423** 70
[25] Mansurov V, Galitsyn Y, Nikitin A, Kolosovsky E, Zhuravlev K, Osvath Z, Dobos L, Horvath Z and Pecz B 2007 *Phys. Status Solidi* c **4** 2498
[26] Monch W 2001 *Semiconductor Surfaces and Interfaces* (Berlin: Springer)
[27] Northrup J, Di Felice R and Neugebauer J 1997 *Phys. Rev.* B **55** 13878
[28] Miao M, Janotti A and Van de Walle C 2009 *Phys. Rev.* B **80** 155319
[29] Reddy P *et al* 2016 *J. Appl. Phys.* **119** 145702
[30] Rosa A and Neugebauer J 2006 *Phys. Rev.* B **73** 205314-1
[31] Kempisty P, Strak P, Sakowski K and Krukowski S 2014 *J. Cryst. Growth* **390** 71
[32] Zhang Z, Hua M, He J, Tang G, Qian Q and Chen K 2018 *Appl. Phys. Express* **11** 081003
[33] Warren W, Kanicki J, Robertson J, Poindexter E and McWhorter P 1993 *J. Appl. Phys.* **74** 4034
[34] Pacchioni G and Erbetta D 1999 *Phys. Rev.* B **60** 12617
[35] Zhuravlev K *et al* 2017 *Semiconductors* **51** 379
[36] Koley G, Tilak V, Eastman L and Spencer M 2003 *IEEE Trans. Electron Devices* **50** 886
[37] Joh J and Del Alamo J 2011 *IEEE Trans. Electron Devices* **58** 132